

# Current-induced near-field radiative energy, linear-momentum, and angular-momentum transfer

Huimin Zhu,<sup>1,4</sup> Gaomin Tang,<sup>2,\*</sup> Lei Zhang,<sup>1,4,†</sup> and Jun Chen<sup>3,4,‡</sup>

<sup>1</sup>State Key Laboratory of Quantum Optics and Quantum Optics Devices,  
Institute of Laser Spectroscopy, Shanxi University, Taiyuan 030006, China

<sup>2</sup>Graduate School of China Academy of Engineering Physics, Beijing 100193, China

<sup>3</sup>State Key Laboratory of Quantum Optics and Quantum Optics Devices,  
Institute of Theoretical Physics, Shanxi University, Taiyuan 030006, China

<sup>4</sup>Collaborative Innovation Center of Extreme Optics, Shanxi University, Taiyuan 030006, China

In this work, we study the near-field radiative energy, linear-momentum, and angular-momentum transfer from a current-biased graphene to nanoparticles. The electric current through the graphene sheet induces nonequilibrium fluctuations, causing energy and momentum transfer even in the absence of a temperature difference. The inherent spin-momentum locking of graphene surface plasmon polaritons leads to an in-plane torque perpendicular to the electric current. In the presence of a temperature difference, energy transfer is greatly enhanced while the lateral force and torque remains within the same order. Our work explores the potential of utilizing current-biased graphene to manipulate nanoparticles.

## I. INTRODUCTION

The inclusion of nonreciprocal effects in the study of near-field thermal radiation has led to the discovery of various novel phenomena and has attracted significant scientific interest<sup>1–9</sup>. Nonreciprocity can be achieved in various scenarios. One example is by applying a magnetic field to magneto-optic materials<sup>1–6</sup>. Another approach is to use magnetic Weyl semimetals that have intrinsic time-reversal symmetry breaking<sup>10–13</sup>.

Nonreciprocity-induced lateral force has been studied recently<sup>14–17</sup>. It has been found that the equilibrium lateral force in nonreciprocal systems can be used for propulsion<sup>14</sup>. Furthermore, it has been discovered<sup>15</sup> that when at least one of the interacting surfaces is made of nonreciprocal materials, materials with different temperatures can experience a nonequilibrium lateral force in the direction parallel to the surfaces. In the case where some part of the system is affected by mobile carrier drift, an atom or nanoparticle placed above the sample with mobile carrier drift experiences a fluctuation force<sup>17</sup>.

Current-biased graphene is also known for its nonreciprocity<sup>18–21</sup>. The exceptional electron mobility of graphene allows it to sustain nonreciprocal surface plasmon polaritons when driven by a current with drift velocity, which gives rise to interesting properties such as Fizeau drag<sup>22,23</sup> and negative Landau damping<sup>24</sup>. Current-biased graphene is in a nonequilibrium state and this leads to a finite photonic chemical potential<sup>25</sup> that depends on the in-plane wave vector for the thermal electromagnetic radiation. The occupation number of radiative photons is nonreciprocal, that is asymmetric with respect to the positive and negative in-plane wave vectors<sup>26–29</sup>. The nonreciprocal properties of current-biased graphene can be adjusted through chemical doping or gate voltage, making it suitable for a wide range of applications in controlling thermal radiation. For example, near-field radiative heat transfer has been studied between two suspended graphene sheets<sup>30</sup>, graphene covered substrates<sup>31</sup>, graphene-nanoparticles<sup>32</sup>, and graphene-based multilayer systems<sup>33</sup>. However, the physical aspects of the force and torque experience by the nanoparticle near the current-biased graphene remain unexplored to date.

In this work, we investigate the near-field transfer of energy, linear momentum, and angular momentum between an isotropic dipolar nanoparticle and the current-biased graphene. The nonequilibrium state in the current-biased graphene induces energy transfer between the particle and the graphene even in the absence of a temperature difference. Importantly, these SPPs carry both linear and spin-locked angular momentum. As a result, there is an exchange of net linear and spin angular momentum between the particle and the SPPs, leading to both lateral force and torque experienced by the nanoparticle.

## II. SYSTEM AND FORMALISM

The system is illustrated schematically in Fig. 1(a), where the spherical nanoparticle with radius  $R$  is placed near the surface of current-biased monolayer graphene. Without losing generality, we assume that the drift velocity  $v_d$  in graphene is along the positive direction of the  $x$  axis. Within the framework of fluctuational electrodynamics, the total power  $H$ , lateral force along  $x$ -direction  $F_x$ , and torque along  $y$ -direction  $M_y$  can be expressed as

$$P = \int_0^\infty \frac{d\omega}{2\pi} p(\omega) \quad (1)$$

with  $P \in \{H, F_x, M_y\}$  and  $p \in \{h, f_x, m_y\}$ . The spectral densities are given by<sup>15</sup>:

$$h(\omega) = -\hbar\omega k_0^2 \text{Im}[\alpha(\omega)] \int \frac{d^2\mathbf{q}}{4\pi^2} \Theta(\omega, \mathbf{q}) \delta n(\omega, q_x), \quad (2)$$

$$f_x(\omega) = \hbar k_0^2 \text{Im}[\alpha(\omega)] \int \frac{d^2\mathbf{q}}{4\pi^2} q_x \Theta(\omega, \mathbf{q}) \delta n(\omega, q_x), \quad (3)$$

$$m_y(\omega) = -\hbar \text{Im}[\alpha(\omega)] \int \frac{d^2\mathbf{q}}{4\pi^2} q_x \text{Im}(r_p e^{2i\beta_0 d}) \delta n(\omega, q_x), \quad (4)$$

with

$$\Theta(\omega, \mathbf{q}) = \text{Re} \left[ \frac{r_p e^{2i\beta_0 d}}{2\beta_0} \left( \frac{2q^2}{k_0^2} - 1 \right) \right]. \quad (5)$$

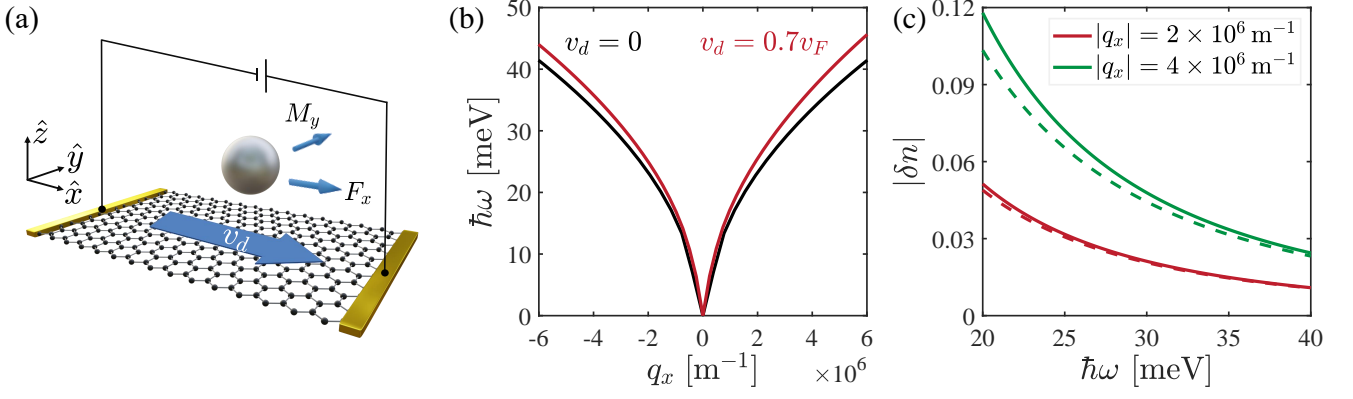


FIG. 1. (a) Schematic plot of the lateral force and torque exerted on an isotropic dipolar particle above a current-biased graphene in the near-field regime. The drift velocity  $v_d$  is along the  $x$  direction. (b) Dispersion of the surface plasmon polaritons of the current-biased graphene. At large drift velocities, the drift current effectively drags the SPPs, leading to the nonreciprocal propagation of SPPs. (c) The absolute value of photon occupation number difference  $|\delta n(\omega, q_x)|$  versus  $\omega$  with  $v_d = 0.7v_F$ . The solid and dashed lines are for positive  $\delta n(\omega, q_x)$  for  $q_x > 0$  and negative  $\delta n(\omega, q_x)$  for  $q_x < 0$ , respectively.

Here,  $r_p$  is the Fresnel reflection coefficient for  $p$  polarization. The in-plane wave vector and the angular frequency are denoted by  $\mathbf{q} = (q_x, q_y)$  and  $\omega$ . The magnitude of the out-of-plane wave vector in air is  $\beta_0 = \sqrt{k_0^2 - q^2}$  with  $k_0 = \omega/c$  and  $q = |\mathbf{q}|$ . The photon-occupation difference between the nanoparticle and the graphene is<sup>26–28</sup>

$$\delta n(\omega, q_x) = [e^{\hbar(\omega - q_x v_d)/k_B T_e} - 1]^{-1} - [e^{\hbar\omega/k_B T_p} - 1]^{-1}, \quad (6)$$

where  $T_e$  and  $T_p$  represent the temperatures of graphene and the nanoparticle, respectively. Equation (6) indicates that the electric current-induced nonequilibrium fluctuations can produce a finite energy flux even in the absence of a temperature difference. In the following, we assume that the temperature of the particle and the graphene is the same with  $T_p = T_e = T = 300$  K, unless there is a special account for the temperatures. The energy transmission function of the energy flux in Eq.(2) is defined as:

$$\mathcal{Z}(\omega, \mathbf{q}) = -\frac{1}{4\pi^2} \hbar\omega k_0^2 \text{Im}[\alpha(\omega)] \Theta(\omega, \mathbf{q}) \delta n(\omega, q_x), \quad (7)$$

which gives the energy transfer at given  $\omega$  and  $\mathbf{q}$ .

The dispersion relation of SPPs in a monolayer graphene can be obtained through the following relation<sup>34</sup>:

$$2i\omega\varepsilon_0 = \beta_0\sigma_g, \quad (8)$$

where the surface conductivity  $\sigma_g$  is given by<sup>35</sup>

$$\sigma_g(\omega, q_x, q_y) = \frac{ie_0^2\omega}{q^2} \frac{\mu(T)}{(\pi\hbar v_F)^2} \int_0^{2\pi} d\theta \frac{1}{(1 - \cos\theta v_d/v_F)^2} \times \frac{q_x(\cos\theta - v_d/v_F) + q_y \sin\theta}{(\hbar\omega + i\gamma)/(\hbar v_F) - q_x \cos\theta - q_y \sin\theta}, \quad (9)$$

with  $\mu(T) = 2k_B T \ln[2 \cosh(\mu_g/2k_B T)]$ . Here,  $T$  is the temperature,  $\mu_g$  is the chemical potential,  $\gamma$  the damping parameter, and  $e_0$  the electron charge. In the numerical calculation, we set the Fermi velocity  $v_F = 10^6$  m/s, the chemical potential  $\mu_g = 0.1$  eV and the damping parameter  $\gamma = 3.7$  meV.

Figure 1(b) shows the nonreciprocal dispersions of SPPs in the presence of an electric current.

### III. NUMERICAL RESULTS

Before considering nonequilibrium energy and momentum transfer, we first discuss the nonreciprocal properties of  $\delta n(\omega, q_x)$  shown in Fig. 1(c). We observe that the photon occupation number difference  $\delta n(\omega, q_x)$  is positive for positive  $q_x$  under  $\omega > q_x v_d$ . This indicates that the effective photonic temperature of the graphene is higher than the particle temperature  $T_p$ . Furthermore, it should be noted that contributions from  $\omega < q_x v_d$  can be disregarded. This is because these contributions become significant only when the separation between the particle and the graphene reaches subnanometer scales<sup>28</sup>, whereas in our case, the distance is on the order of micrometers. Consequently, photons, especially those with positive  $q_x$ , flow from the graphene to the particle. In contrast, for negative  $q_x$ ,  $\delta n(\omega, q_x)$  is always negative. Therefore, the effective photonic temperature of the graphene is lower than  $T_p$ . This sign reversal indicates a reversal in the direction of photon transfer compared to the behavior exhibited by positive  $q_x$ .

We analyze three kinds of nanoparticle: NaCl, undoped GaAs, and InSb. The intricate dielectric characteristics are given by the well-established Lorentz-Drude model with<sup>36,37</sup>

$$\varepsilon(\omega) = \varepsilon_\infty \frac{\omega_L^2 - \omega^2 - i\Gamma\omega}{\omega_T^2 - \omega^2 - i\Gamma\omega}, \quad (10)$$

where  $\varepsilon_\infty$  is the high-frequency dielectric constant,  $\omega_L$  is the longitudinal optic-phonon frequency,  $\omega_T$  is the transverse optic-phonon frequency,  $\Gamma$  is the optic-phonon damping constant. Within the electrostatic limit, we can reasonably neglect multiple scattering interactions between the particle and the graphene, and describe the particle effectively using its electrical polarizability which is expressed as  $\alpha(\omega) = 4\pi R^3 [\varepsilon(\omega) -$

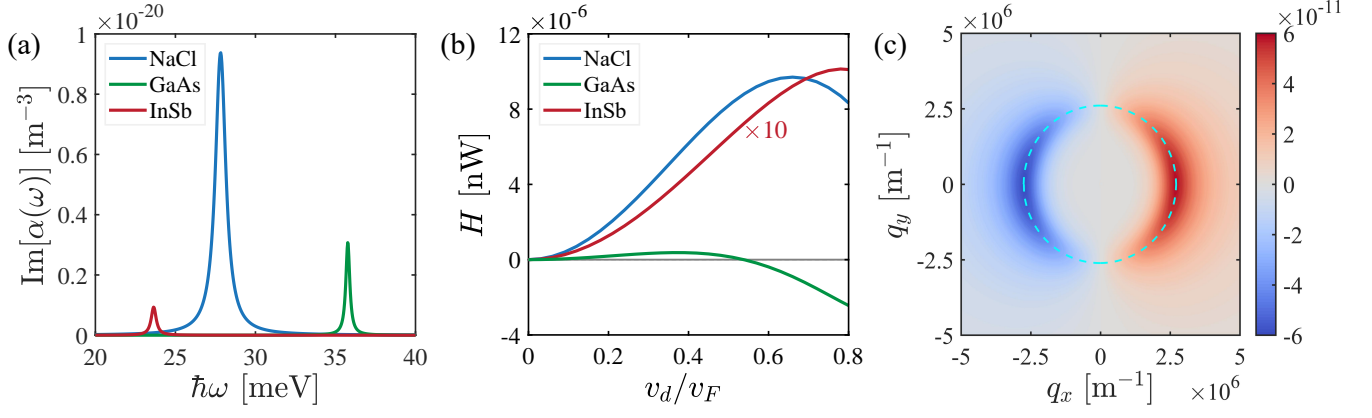


FIG. 2. (a) Imaginary part of the polarizability for different nanoparticles with radius  $R = 40$  nm. (b) Net power transfer experienced by nanoparticles as a function of  $v_d$  at a fixed separation distance of  $d = 0.2 \mu\text{m}$ . The curve for the InSb particle is multiplied by a factor of 10 for better visibility. (c) Energy transmission function  $\mathcal{Z}$  (in units of  $\text{nJ}\cdot\text{nm}^2$ ) plotted against  $q_x$  and  $q_y$  at  $v_d = 0.3v_F$ ,  $d = 0.2 \mu\text{m}$ , and  $\hbar\omega = 27.8 \text{ meV}$ . The cyan dashed line represents the dispersion of graphene SPPs.

$1)/[\varepsilon(\omega) + 2]^{38}$ . It is important to note that these assumptions are valid only under specific conditions:  $R \ll d \ll \hbar c/k_B T$ . In Fig. 2(a), we present the imaginary part of the polarizability for these nanoparticles, revealing distinct dipolar resonances.

Now we study the effect of drift velocity on the net power transfer experienced by different nanoparticles, as shown in Fig. 2(b). We differentiate between positive and negative energy fluxes, which represent the flow of energy from the graphene to the particle and from the particle to the graphene, respectively. Our analysis reveals intriguing behaviors. For NaCl and InSb particles, the power transfer initially increases as  $v_d$  increases. However, with increasing  $v_d$  further, the power transfer decreases. In contrast, the direction of net power transfer undergoes a change for GaAs particles as the drift velocity increases. These are due to the interplay between the nonreciprocal properties of the SPPs and photonic occupation number of graphene.

To analyze the contributions of forward ( $q_x > 0$ ) and backward ( $q_x < 0$ ) SPPs to net power transfer, we use the NaCl particle as an example. In Fig. 2(c), we show the energy transmission function and the dispersion of graphene plasmons (represented by the cyan dashed line). This visual representation aligns the bright branches of the energy transmission function with the cyan dashed line, confirming the dominant role played by SPPs in governing power transfer in our system. For  $q_x > 0$ , the energy transfer coefficients are positive, indicating energy transfer from graphene to the particle. For  $q_x < 0$ , the energy transfer coefficients are negative, signifying energy transfer from the particle back to the graphene. Therefore, the net energy transfer is the sum of contributions from  $q_x > 0$  and  $q_x < 0$ . At lower drift velocities, the nonreciprocal characteristics of SPPs are not pronounced, and energy transfer is mainly governed by the nonreciprocal photon occupation number difference  $\delta n(\omega, q_x)$ , as shown in Fig. 1(c). However, as the drift velocity increases, nonreciprocal SPPs gradually interact with  $\delta n(\omega, q_x)$ . The high drift velocity suppresses the net power transfer caused by the nonreciprocal photon occupation num-

ber, resulting in a decrease in energy transfer between NaCl, InSb, and graphene, and shifts in energy transfer direction observed between GaAs and graphene.

Subsequently, we investigate the effect of drift velocity on linear-momentum and angular-momentum transfer between particles and the graphene. We define positive  $M_y$  as directed along the negative  $y$ -axis and positive  $F_x$  as oriented in the positive  $x$ -axis direction. Our findings revealed a consistent trend: both force [Fig. 3(a)] and torque [Fig. 3(b)] initially increase with an increment in drift velocity ( $v_d$ ), irrespective of the particle's material. However, at higher  $v_d$  values, these quantities tend to decrease. This trend is consistent with the energy transfer.

To gain a deeper understanding of the force and torque dynamics acting on the particle, we analyze the exchange of linear momentum and spin angular momentum between the forward ( $q_x > 0$ ) and backward ( $q_x < 0$ ) SPPs and the particle. When photons transfer from the graphene to the particle ( $q_x > 0$ ), the particle gains momentum, contributing to the lateral force along the positive  $x$  direction. Conversely, when  $q_x < 0$ , the particle loses momentum due to the reverse photon transfer, producing a lateral force in the same direction. Therefore, SPPs with both positive and negative  $q_x$  generate a net lateral force directed along the positive  $x$  direction. Due to the spin-momentum lock of SPPs<sup>39</sup>, the transverse spin of SPPs strongly couples with their propagation direction. As a result, when SPPs propagate in the positive (negative)  $x$  direction, their spin aligns with the negative (positive)  $y$  direction, respectively. This spin angular momentum transfer is facilitated by photon tunneling from the graphene to the particle in the case of  $q_x > 0$ , generating a torque directed along the negative  $y$  direction. Importantly, the torque stemming from  $q_x < 0$  contributions also points in the same negative  $y$  direction. Consequently, polaritons in both positive and negative  $q_x$  directions collectively generate a net lateral torque along the negative  $y$  direction. The consistency of these findings is supported by Fig. 3(c), which depicts the torque spectral

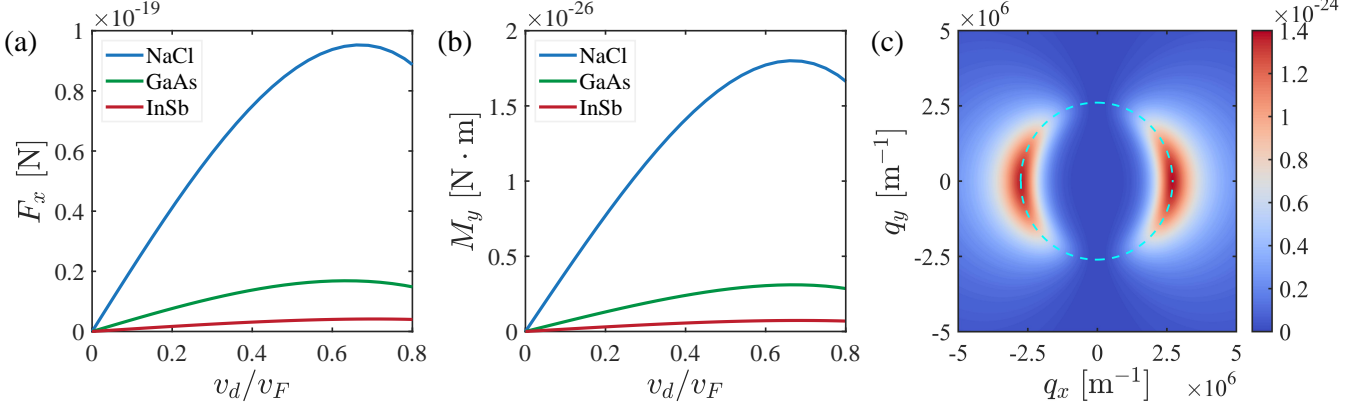


FIG. 3. (a) Net force on different nanoparticles as a function of  $v_d$  at  $d = 0.2 \mu\text{m}$ . (b) Net torque as a function of  $v_d$  at  $d = 0.2 \mu\text{m}$ . (c) Torque spectral density  $m_y$  (in  $\text{nJ}\cdot\text{nm}^2\cdot\text{s}$ ) as a function of  $q_x$  and  $q_y$  at  $\hbar\omega = 27.8 \text{ meV}$  and  $v_d = 0.3v_F$ . The cyan dashed line represents the dispersion of graphene SPPs.

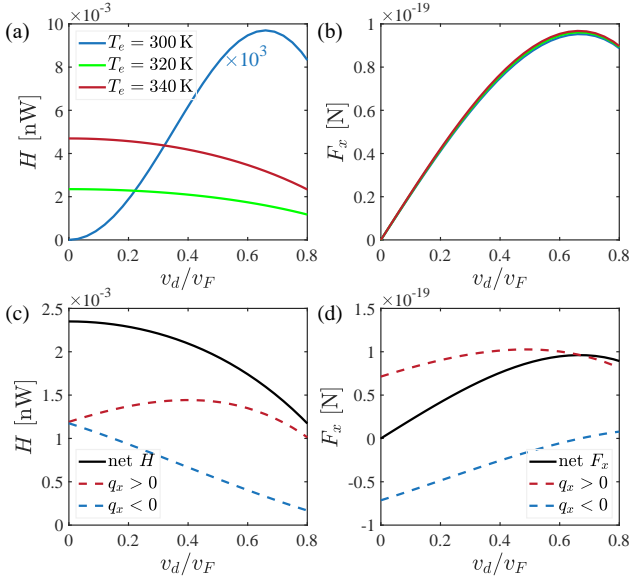


FIG. 4. (a) Net power and (b) force for the NaCl particle as a function of  $v_d$  at various graphene temperatures  $T_e$ , with  $T_p = 300 \text{ K}$  and  $d = 0.2 \mu\text{m}$ . The power transfer curve at  $T_e = 300 \text{ K}$  is multiplied by  $10^3$  for better visibility. (c) Net power and (d) force versus  $v_d$  with  $T_p = 300 \text{ K}$  and  $T_e = 320 \text{ K}$ . Its characteristic shape follows from the collective contributions of forward ( $q_x > 0$ ) and backward ( $q_x < 0$ ) SPPs, which are plotted separately as dashed lines.

density  $m_y$  as a function of  $q_x$  and  $q_y$  at  $\hbar\omega = 27.8 \text{ meV}$  and  $v_d = 0.3v_F$ . Notably, for both positive and negative  $q_x$ , the torque spectral density  $m_y$  consistently maintains positive values, aligning closely with the dispersion curve of graphene plasmons. Remarkably, the force and torque induced by current-biased graphene are on par with those in thermally excited nonreciprocal surface electromagnetic waves<sup>15</sup>.

Finally, we consider the scenario where the temperature of the particle differs from that of the graphene. Figure 4(a-b)

shows the dependence of net energy transfer and lateral force on the NaCl particle with a radius of  $R = 40 \text{ nm}$  at various temperatures of the graphene, while the temperature of the particle remains at  $300 \text{ K}$ . Interestingly, the energy transfer from the graphene to the NaCl particle increases by three orders of magnitude. To explain this, we calculate both the forward and backward SPPs that contribute to the energy and momentum transfer from the graphene to the particle in the case of  $T_e > T_p$ . The numerical results are presented in Fig. 4(c,d). From Fig. 4(c), we observe that the energy transfer for photons with opposite momentum has the same sign, which is completely different from the case when the temperatures are equal. Therefore, the energy transfer is greatly enhanced when a temperature difference is introduced. In contrast, we observe that the photons with  $q_x > 0$  and  $q_x < 0$  make positive and negative contributions to the force, respectively. By summing up the contributions from all photons, we find that the force experienced by the particle does not differ significantly from that in the equal temperature case. As a result, the temperature difference has minimal impact on the lateral force while significantly enhancing the net power transfer between the graphene and the particle.

#### IV. CONCLUSION

We have investigated the near-field radiative energy, linear-momentum, and angular-momentum transfer from a current-biased graphene sheet to nanoparticles. Notably, for the GaAs particle, both the magnitude and the direction of energy transfer can be electrically manipulated. This unique phenomenon results from the interplay of nonreciprocal photon occupation differences and graphene surface plasmon polaritons. Moreover, in the presence of a temperature difference, our study reveals distinct energy transfer behavior while maintaining consistent force characteristics compared to the scenario without temperature difference.

## ACKNOWLEDGMENTS

H.Z., L.Z., and J.C. acknowledge the support from the National Natural Science Foundation of China (Grant No. 12074230, 12174231), the Fund for Shanxi “1331 Project”, Fundamental Research Program of Shanxi Province through 202103021222001, Program of Education and Teaching Reform in Shanxi Province [Grant No. J20230003], Re-

search Project Supported by Shanxi Scholarship Council of China. G.T. is supported by National Natural Science Foundation of China (No. 12374048, 12088101) and NSAF (No. U2330401). This research was partially conducted using the High Performance Computer of Shanxi University.

\*gmtang@gscaep.ac.cn

†zhanglei@sxu.edu.cn

‡chenjun@sxu.edu.cn

- <sup>1</sup> E. Moncada-Villa, V. Fernández-Hurtado, F. J. García-Vidal, A. García-Martín, and J. C. Cuevas, “Magnetic field control of near-field radiative heat transfer and the realization of highly tunable hyperbolic thermal emitters,” *Phys. Rev. B* **92**, 125418 (2015).
- <sup>2</sup> P. Ben-Abdallah, “Photon thermal Hall effect,” *Phys. Rev. Lett.* **116**, 084301 (2016).
- <sup>3</sup> Linxiao Zhu and Shanhui Fan, “Persistent directional current at equilibrium in nonreciprocal many-body near field electromagnetic heat transfer,” *Phys. Rev. Lett.* **117**, 134303 (2016).
- <sup>4</sup> Ivan Latella and Philippe Ben-Abdallah, “Giant Thermal Magnetoresistance in Plasmonic structures,” *Phys. Rev. Lett.* **118**, 173902 (2017).
- <sup>5</sup> Ricardo M. Abraham Ekeröth, Philippe Ben-Abdallah, Juan Carlos Cuevas, and Antonio García-Martín, “Anisotropic thermal magnetoresistance for an active control of radiative heat transfer,” *ACS Photonics* **5**, 705–710 (2018).
- <sup>6</sup> Annika Ott and Svend-Age Biehs, “Thermal rectification and spin-spin coupling of nonreciprocal localized and surface modes,” *Phys. Rev. B* **101**, 155428 (2020).
- <sup>7</sup> Gaomin Tang, Jun Chen, and Lei Zhang, “Twist-induced control of near-field heat radiation between magnetic Weyl semimetals,” *ACS Photonics* **8**, 443–448 (2021).
- <sup>8</sup> Gaomin Tang, Lei Zhang, Yong Zhang, Jun Chen, and C. T. Chan, “Near-Field Energy Transfer between Graphene and Magneto-Optic Media,” *Phys. Rev. Lett.* **127**, 247401 (2021).
- <sup>9</sup> S.-A. Biehs, R. Messina, P. S. Venkataram, A. W. Rodriguez, J. C. Cuevas, and P. Ben-Abdallah, “Near-field radiative heat transfer in many-body systems,” *Rev. Mod. Phys.* **93**, 025009 (2021).
- <sup>10</sup> Bo Zhao, Cheng Guo, Christina A. C. Garcia, Prineha Narang, and Shanhui Fan, “Axion-field-enabled nonreciprocal thermal radiation in Weyl semimetals,” *Nano Lett.* **20**, 1923–1927 (2020).
- <sup>11</sup> Cheng Guo, Bo Zhao, Danhong Huang, and Shanhui Fan, “Radiative thermal router based on tunable magnetic Weyl semimetals,” *ACS Photonics* **7**, 3257–3263 (2020).
- <sup>12</sup> Yoichiro Tsurimaki, Xin Qian, Simo Pajovic, Fei Han, Mingda Li, and Gang Chen, “Large nonreciprocal absorption and emission of radiation in type-I Weyl semimetals with time reversal symmetry breaking,” *Phys. Rev. B* **101**, 165426 (2020).
- <sup>13</sup> Simo Pajovic, Yoichiro Tsurimaki, Xin Qian, and Gang Chen, “Intrinsic nonreciprocal reflection and violation of Kirchhoff’s law of radiation in planar type-I magnetic Weyl semimetal surfaces,” *Phys. Rev. B* **102**, 165417 (2020).
- <sup>14</sup> David Gelbwaser-Klimovsky, Noah Graham, Mehran Kardar, and Matthias Krüger, “Near Field Propulsion Forces from Nonreciprocal Media,” *Phys. Rev. Lett.* **126**, 170401 (2021).
- <sup>15</sup> Chinmay Khandekar, Siddharth Buddhiraju, Paul R. Wilkinson, James K. Gimzewski, Alejandro W. Rodriguez, Charles Chase, and Shanhui Fan, “Nonequilibrium lateral force and torque by thermally excited nonreciprocal surface electromagnetic waves,” *Phys. Rev. B* **104**, 245433 (2021).
- <sup>16</sup> Yoichiro Tsurimaki, Renwen Yu, and Shanhui Fan, “Moving media as photonic heat engine and pump,” *Phys. Rev. B* **107**, 115406 (2023).
- <sup>17</sup> Boris Shapiro, “Fluctuation-induced forces in the presence of mobile carrier drift,” *Phys. Rev. B* **96**, 075407 (2017).
- <sup>18</sup> Dan S. Borgnia, Trung V. Phan, and Leonid S. Levitov, “Quasi-relativistic doppler effect and non-reciprocal plasmons in graphene,” (2015), arXiv:1512.09044.
- <sup>19</sup> Ben Van Duppen, Andrea Tomadin, Alexander N Grigorenko, and Marco Polini, “Current-induced birefringent absorption and non-reciprocal plasmons in graphene,” *2D Materials* **3**, 015011 (2016).
- <sup>20</sup> Tiago A. Morgado and Mário G. Silveirinha, “Drift-induced unidirectional graphene plasmons,” *ACS Photonics* **5**, 4253–4258 (2018).
- <sup>21</sup> Tiago A. Morgado and Mário G. Silveirinha, “Nonlocal effects and enhanced nonreciprocity in current-driven graphene systems,” *Phys. Rev. B* **102**, 075102 (2020).
- <sup>22</sup> Y. Dong, L. Xiong, I. Y. Phinney, Z. Sun, R. Jing, A. S. McLeod, S. Zhang, S. Liu, F. L. Ruta, H. Gao, Z. Dong, R. Pan, J. H. Edgar, P. Jarillo-Herrero, L. S. Levitov, A. J. Millis, M. M. Fogler, D. A. Bandurin, and D. N. Basov, “Fizeau drag in graphene plasmonics,” *Nature* **594**, 513–516 (2021).
- <sup>23</sup> Wenyu Zhao, Sihan Zhao, Hongyuan Li, Sheng Wang, Shaoxin Wang, M. Iqbal Bakti Utama, Salman Kahn, Yue Jiang, Xiao Xiao, SeokJae Yoo, Kenji Watanabe, Takashi Taniguchi, Alex Zettl, and Feng Wang, “Efficient Fizeau drag from Dirac electrons in monolayer graphene,” *Nature* **594**, 517–521 (2021).
- <sup>24</sup> Tiago A. Morgado and Mário G. Silveirinha, “Negative Landau damping in bilayer graphene,” *Phys. Rev. Lett.* **119**, 133901 (2017).
- <sup>25</sup> Charles H. Henry and Rudolf F. Kazarinov, “Quantum noise in photonics,” *Rev. Mod. Phys.* **68**, 801–853 (1996).
- <sup>26</sup> A. I. Volokitin and B. N. J. Persson, “Theory of the interaction forces and the radiative heat transfer between moving bodies,” *Phys. Rev. B* **78**, 155437 (2008).
- <sup>27</sup> A. I. Volokitin and B. N. J. Persson, “Quantum friction,” *Phys. Rev. Lett.* **106**, 094502 (2011).
- <sup>28</sup> A. I. Volokitin and B. N. J. Persson, “Near-field radiative heat transfer between closely spaced graphene and amorphous SiO<sub>2</sub>,” *Phys. Rev. B* **83**, 241407(R) (2011).
- <sup>29</sup> Jiebin Peng and Jian-Sheng Wang, “Current-induced heat transfer in double-layer graphene,” arXiv:1805.09493.
- <sup>30</sup> Yong Zhang, Cheng-Long Zhou, Lei Qu, and Hong-Liang Yi, “Active control of near-field radiative heat transfer through non-reciprocal graphene surface plasmons,” *Appl. Phys. Lett.* **116**, 151101 (2020).
- <sup>31</sup> Kezhang Shi, Zhaoyang Chen, Yuxin Xing, Jianxin Yang, Xinan Xu, Julian S. Evans, and Sailing He, “Near-Field Radiative Heat

- Transfer Modulation with an Ultrahigh Dynamic Range through Mode Mismatching,” *Nano Lett.* **22**, 7753–7760 (2022).
- <sup>32</sup> Yong Zhang, Cheng-Long Zhou, Hong-Liang Yi, and He-Ping Tan, “Radiative thermal diode mediated by nonreciprocal graphene plasmon waveguides,” *Phys. Rev. Appl.* **13**, 034021 (2020).
- <sup>33</sup> Cheng-Long Zhou, Lei Qu, Yong Zhang, and Hong-Liang Yi, “Enhancement and active mediation of near-field radiative heat transfer through multiple nonreciprocal graphene surface plasmons,” *Phys. Rev. B* **102**, 245421 (2020).
- <sup>34</sup> P A D Gonçalves and N M R Peres, *An Introduction to Graphene Plasmonics* (WORLD SCIENTIFIC, 2016).
- <sup>35</sup> Dmitry Svintsov and Victor Ryzhii, “Comment on “Negative Landau damping in bilayer graphene”,” *Phys. Rev. Lett.* **123**, 219401 (2019).
- <sup>36</sup> Stavroula Foteinopoulou, Ganga Chinna Rao Devarapu, Ganapathi S Subramania, Sanjay Krishna, and Daniel Wasserman, “Phonon-polaritonics: enabling powerful capabilities for infrared photonics,” *Nanophotonics* **8**, 2129–2175 (2019).
- <sup>37</sup> Chinmay Khandekar and Zubin Jacob, “Thermal spin photonics in the near-field of nonreciprocal media,” *New J. Phys.* **21**, 103030 (2019).
- <sup>38</sup> Rongkuo Zhao, Alejandro Manjavacas, F Javier Garcia de Abajo, and JB Pendry, “Rotational Quantum Friction,” *Phys. Rev. Lett.* **109**, 123604 (2012).
- <sup>39</sup> Konstantin Y Bliokh, Daria Smirnova, and Franco Nori, “Quantum spin Hall effect of light,” *Science* **348**, 1448–1451 (2015).